Ultra-Short-Range, Precise Displacement Measurement Setup with a Near Field Slot-Line Antenna and a Dedicated Spiral Calibration

Sarah Linz, Fabian Lurz, Michael Sporer, Stefan Lindner, Sebastian Mann,
Robert Weigel, and Alexander Koelpin
Institute for Electronics Engineering, Friedrich-Alexander University of Erlangen-Nuremberg
Cauerstrasse 9, 91058 Erlangen, Germany – sarah.linz@fau.de

***Abstract*—This work introduces a precise measurement setup for displacement analysis in the near field of a tapered slot-line antenna from 0 mm up to 20 mm distance. Enhanced accuracy is achieved by a dedicated spiral reconstruction algorithm accounting for the near field effects. Moreover, the precision of the system in the micrometer range is guaranteed by four synchronous 24 bit analog-to-digital converters and a decimation factor of 10, leading to an overall update rate of 1 kHz.**

***Index Terms*—K-band, industrial positioning, near field measurement, spiral calibration.**

I. Introduction

Since decades, radar systems have been employed for navigation and tracking in civil and military tasks as well as for space-related research. Nowadays, they are also more and more used for industrial positioning and in everyday life. The area of application ranges from low-cost and basic systems, e.g., door openers, to accurate and elaborated radars like tank level gauges.

Common radar systems use mixer-based receivers and a modulation scheme that relates the time-of-flight to the distance of the target, e.g., pulse or frequency modulated continuous wave radar. Already in the 1970s Engen and Hoer proposed the Six-port junction as an alternative reflectometer [1], [2]. In the present work this receiver is used to measure the reflection caused by a target in the near field of a tapered slot-line antenna. Since the reflection is a function of the target's position, the receiver is employed as a radar for near field measurements. An application may be precise industrial positioning and tracking of machinery with displacements from 0 to 20 mm.

An antenna-reflector system for ultra-short-range radars has already been proposed in [3]. However, this system relies on a modified target, that transpolarizes the electromagnetic wave. Thus, it cannot always be integrated in existing machinery for industrial positioning. The system presented here can be applied to any target, reflecting 24 GHz signals.

Frequency modulated continuous wave radar systems with very high precision in the micrometer range rely on a very wide bandwidth. In [4], for instance, a bandwidth of 25.6 GHz around the center frequency 80 GHz is necessary to achieve a standard deviation of 0.36 µm (100 measurement values at one fixed position). However, the applications of such ultra-wide bandwidth radars are very limited due to regulatory requirements. The presented system is operated in the ISM band at 24 GHz with a single frequency continuous wave and therefore the use for industrial, scientific and medical applications is not limited to enclosed environments.

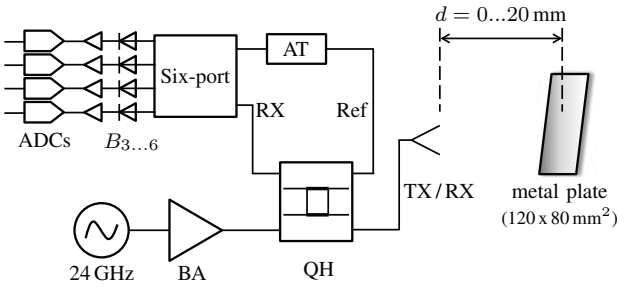

Fig. 1. Block diagram of the system (BA: buffer amplifier, QH: quadrature hybrid, AT: attenuator).

The magnitude in the near field of an antenna strongly declines with the distance. Therefore, the received signals' magnitudes also show an exponential drop over the displacement in the near field and a spiral characteristic in the complex plane as demonstrated in [5].

In the following, the Six-port based measurement setup is presented and compared to a conventional vector network analyzer. An enhanced accuracy is achieved by a dedicated calibration routine each $\lambda/2$ displacement to reduce the near field effects in the measurement data.

II. System Concept

The concept of the ultra-short-range radar is illustrated by a block diagram in Fig. 1. The RF front-end has been presented in [6] together with a microstrip to parallel-plate waveguide transition for displacement measurement in the waveguide's fringing field.

A phase-locked loop stabilized voltage controlled oscillator and a buffer amplifier (BA) are used to avoid de-tuning due to the target's position. The 24 GHz continuous wave signal is fed through a quadrature hybrid (QH) to the antenna as transmit signal (TX) and to the Six-port receiver as reference (Ref) signal. The electromagnetic wave, that is reflected from the target and received by the antenna, is fed in reverse direction through the same quadrature hybrid to the second input port of the Six-port network as received (RX) signal. An additional quadrature hybrid (AT) in the reference path is terminated at two ports by one resistor in each branch for attenuating the reference signal and adapting the power level to the received signal.

The Six-port network comprises three quadrature hybrids and one Wilkinson power divider similar to the configuration in [7]. At the four output ports, the power levels are converted to baseband voltages by Schottky diode power detectors with square-law characteristic. The resulting voltages $B_{3...6}$ are amplified and sampled by four synchronous 24 bit analog-to-digital converters (ADCs). A sampling rate of 10 kHz and decimation factor of 10 results in a measurement value update rate of 1 kHz. The signal processing is done on a laboratory computer in Matlab.

When using the Six-port as a network analyzer, $B_{3...6}$ represent the differential in-phase (I) and quadrature (Q) components of the input reflection $\underline{S}_{11}$ of a device under test:

$$\underline{S}_{11} = I + \mathrm{j}Q = (B_5 - B_6) + \mathrm{j}(B_3 - B_4) \tag{1}$$

By connecting an antenna to one input port of the Six-port receiver and observing a target in the far field of the antenna, the distance between target and antenna modulates the phase φ of $\underline{S}_{11}$. Thus, the displacement Δd of the target can be measured by evaluating the phase variation $\Delta\varphi$ [6]:

$$\Delta\varphi = \arg\left\{\underline{S}_{11}\left(\Delta d\right)\right\} = \tan^{-1}\left(\frac{B_3 - B_4}{B_5 - B_6}\right), \tag{2}$$

$$\Delta d = \Delta\varphi\frac{\lambda}{4\pi}, \tag{3}$$

where $\lambda = 12.5$ mm is the free-space wavelength at 24 GHz.

As known from other continuous wave measurement setups, the phase $\Delta\varphi$ exhibits ambiguities. For the proposed displacement measurement, the ambiguity-free range is equal to half of the wavelength. Thus, after a displacement of $\Delta d = 6.25$ mm the phase is wrapped. However, in the near field region of an antenna the field strength is strongly declining. This results also in a modulation of the magnitude of $\underline{S}_{11}$ due to the displacement. It has been proposed in [5] that this modulation can be used to overcome the ambiguity issue. In this work the decline of the field strength is taken into account by a dedicated reconstruction method. The effects of the employed antenna in near field applications will be discussed with the help of measurement results in the following section.

III. Measurement Results

A. Tapered Slot-line Antenna

For characterization purposes the antenna has been separately fabricated on a *Rogers RO4350B* dielectric substrate with thickness $h = 254\,\mu$m and relative permittivity $\varepsilon_r = 3.48$. A photo of the antenna with a transition to microstrip transmission line is depicted in Fig. 2. The tapered slot-line antenna has been measured by the vector network analyzer (VNA) *PNA-X N5244A* from *Keysight Technoliogies* for reference purpose.

The input reflection coefficient at 24 GHz is $|\underline{S}_{11}| = -11$ dB for free space measurements. With the moving target, which is a metal plate (120 x 80 mm^2), in very close vicinity of the antenna, the input reflection coefficient varies in magnitude and phase according to the position of the target. The resulting real (in-phase) and imaginary (quadrature) part of the $\underline{S}_{11}$ is

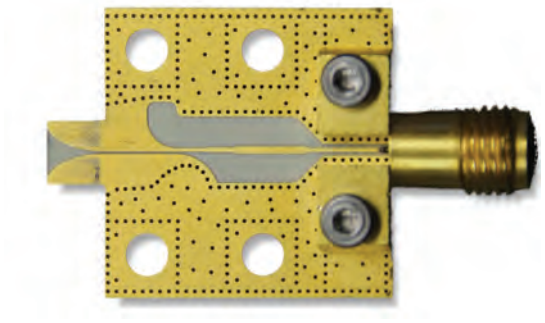

Fig. 2. Photo of slot-line antenna with transition to microstrip transmission line.

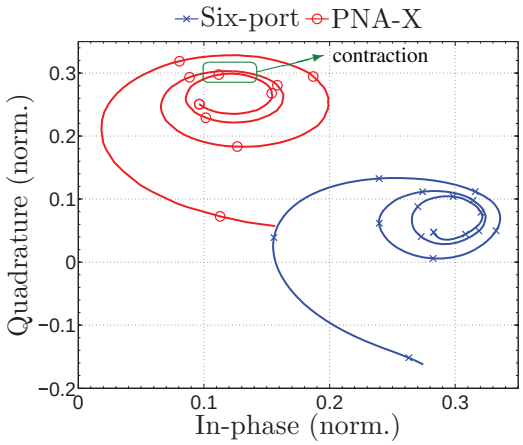

Fig. 3. Measured reflection of the antenna at 24 GHz for target positions from 0 mm to 20 mm.

depicted in Fig. 3, where the reference impedance Z_0 is 50 Ω. For the measurement, the VNA has been calibrated between 20.0 GHz and 26.5 GHz to the plane of the 2.92 mm end-launch cable connector. Thus, the center of the spiral in the complex plane represents the $\underline{S}_{11}$ of the antenna in an anechoic environment.

B. Calibration for Displacement Measurements

For an accurate reconstruction of the target's displacement, the center of the logarithmic, elliptic spiral, describing the antenna's measured input reflection $\widetilde{\underline{S}}_{11}$, has to be moved to the origin of the complex plane. This is equivalent to removing the offset O_I and O_Q of the I/Q signals:

$$\begin{aligned}\widetilde{\underline{S}}_{11} = \widetilde{I} + \mathrm{j}\,\widetilde{Q} &= A_I e^{b\varphi}\cos(\varphi) + O_I \\ &\quad + \mathrm{j}\left[A_Q e^{b\varphi}\sin(\varphi + \phi_Q) + O_Q\right],\end{aligned} \tag{4}$$

where j is the imaginary unit and b the gradient of the amplitudes over the distance. Furthermore, the amplitudes A_I and A_Q have to be equalized and the phase imbalance ϕ_Q has to be compensated [8]. Otherwise, the spiral has an elliptic characteristic causing false results when calculating the phase variation $\Delta\varphi$ with (2) and thus, incorrect displacement values Δd.

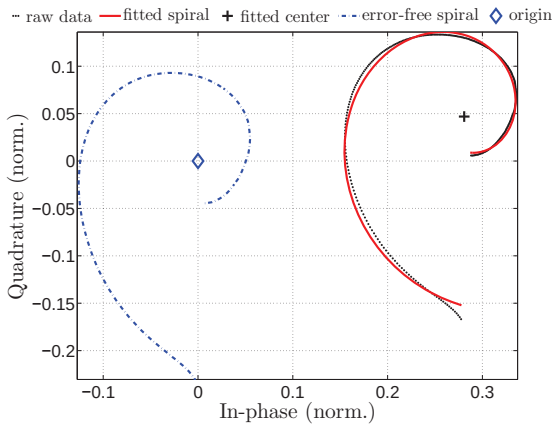

Fig. 4. Measured (black), fitted (red), and calibrated (blue) spiral of measured Six-port data for displacement from 0 to 6.6 mm.

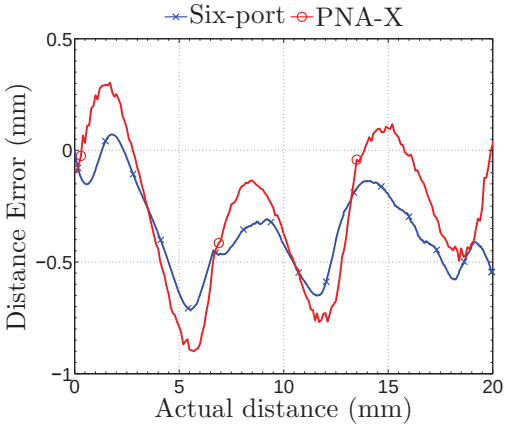

Fig. 5. Error curve comparison of the near field measurement by the proposed Six-port network and the commercial VNA *PNA-X*

The curve of the *PNA-X* measurement at 24 GHz in Fig. 3 shows that the center of the spiral is moving with the displacement. Therefore, a contraction of the measurement values can be noticed in the upper part of the spiral (marked in Fig. 3). In (4), this effect can be modeled as offsets, that are a function of the distance: $O_I(d)$, $O_Q(d)$. The reason for this offset variation is probably a standing wave between target and antenna due to non-ideal receiving characteristics. As a consequence, the measurement data is piecewise approximated by an elliptic spiral according to (4) for each $\lambda/2$ displacement.

The raw data of the Six-port measurement and a fit for a displacement from 0 mm (touching the antenna) to 6.6 mm is shown in Fig. 4. Moreover, the center of the fitted spiral, which corresponds to the offset of the measured I/Q data, is marked with a plus-sign (+). To find the best fit for the spiral, an unconstrained nonlinear optimization algorithm is applied in Matlab. After the fitting, the measurement data's offset is shifted to the origin of the complex plane and the elliptic characteristic is compensated by an equalization of the I and Q signals. The error-compensated spiral is plotted in Fig. 4 with a blue dash-dotted line. On this curve, the reconstruction of the phase variation $\Delta\varphi$ by using (2) can be applied and thus, the calculation of the displacement Δd with (3) is possible.

C. Ultra-short-range Radar

For the evaluation of the system, the target's distance d to the antenna has been swept from 0 mm to 20 mm with 20 µm step size. The displacement of the target has been measured by the proposed Six-port network and the commercial VNA *PNA-X* as a reference system. The I/Q signals are depicted in Fig. 3. It has to be noted, that only the *PNA-X* has been calibrated at the plane of the 2.92 mm connector with a short/open/load calibration kit for S-parameter measurements. Thus, the curve in Fig. 3 directly represents the $\underline{\widetilde{S}}_{11}$ of the antenna in front of a shifting target. However, the Six-port front-end has not been calibrated with short/open/load calibration standards. The baseband voltages $B_{3\ldots6}$ have been normalized (norm.) to the full-scale range of the ADCs to

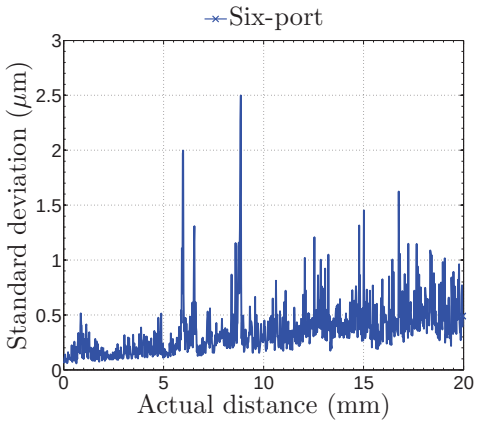

Fig. 6. Standard deviation of the measurement results over the distance between target and antenna.

be plotted in the complex I/Q plane. Only the phase, and therefore also the displacement, can be evaluated after the specific spiral calibration described before.

After the data acquisition, the piecewise spiral reconstruction is applied to the measurement data and the displacement Δd is calculated. In Fig. 5, the accuracy of both measurements is given by the absolute error curve. It can be noticed that the accuracy has a sinusoidal characteristic with a period corresponding to $\lambda/2$ for both measurement setups.

At each position of the target, $n = 2000$ samples have been acquired with the Six-port front-end and an update rate of 1 kHz. The standard deviation σ has been calculated in Matlab according to:

$$\sigma = \sqrt{\frac{1}{n-1}\sum_{i=1}^{n}(x_i - \bar{x})^2}, \tag{5}$$

where x_i are the measurement values and $\bar{x}$ is the mean value at each position. The standard deviation of the measurement data over the actual distance is plotted in Fig. 6. The peaks of the standard deviation that occur over the distance can be

reduced by further increasing the sample size. But even for the sample size of 2000, σ is below 3 µm for all positions and there is only a small increase over the distance. The average standard deviation is below 1 µm.

IV. Conclusion

In this work, a setup for precise displacement measurement in the near field of a tapered slot-line antenna has been discussed. Furthermore, a dedicated calibration algorithm that accounts for the effects caused by the near field characteristic of the antenna has been introduced. A fit of the measurement data for $\lambda/2$ displacements by an elliptic, logarithmic spiral is applied. With the calibrated measurement data, precise displacement detection with a standard deviation of less than 3 µm over the whole measurement range is achieved.

Acknowledgment

The research project "Kurzwegradar" (engl. short-range radar) is supported by the Bavarian Ministry of Economic Affairs and Media, Energy and Technology, Munich, Germany, project grant No. MST-1208-0005// BAY1 75/001.

References

[1] G. F. Engen, "The six-port reflectometer: An alternative network analyzer," *Microwave Theory and Techniques, IEEE Transactions on*, vol. 25, no. 12, pp. 1075–1080, 1977.

[2] C. A. Hoer, *Using six-port and eight-port junctions to measure active and passive circuit parameters*. National Bureau of Standards (U.S.), Sep. 1975.

[3] C. Baer, T. Musch, C. Schulz, B. Will, and I. Rolfes, "A monostatic antenna-reflector system for ultra-short-range radar applications," in *Antennas and Propagation Society International Symposium (APSURSI), 2013 IEEE*, July 2013, pp. 956–957.

[4] N. Pohl, T. Jaeschke, and K. Aufinger, "An ultra-wideband 80 GHz FMCW radar system using a SiGe bipolar transceiver chip stabilized by a fractional-N PLL synthesizer," *Microwave Theory and Techniques, IEEE Transactions on*, vol. 60, no. 3, pp. 757–765, March 2012.

[5] K. Haddadi, M. Wang, D. Glay, and T. Lasri, "A 60 GHz Six-port distance measurement system with sub-millimeter accuracy," *Microwave and Wireless Components Letters, IEEE*, vol. 19, no. 10, pp. 644–646, Oct 2009.

[6] S. Mann, S. Lindner, F. Lurz, F. Barbon, S. Linz, R. Weigel, and A. Koelpin, "A microwave interferometer based contactless quasi-TEM waveguide position encoder with micrometer accuracy," in *Microwave Symposium (IMS), 2014 IEEE MTT-S International*, June 2014, pp. 1–4.

[7] S. Tatu and K. Wu, "Six-port technology and applications," in *Telecommunication in Modern Satellite, Cable and Broadcasting Services (TELSIKS), 2013 11th International Conference on*, vol. 01, Oct 2013, pp. 239–248.

[8] A. Singh, X. Gao, E. Yavari, M. Zakrzewski, X. H. Cao, V. Lubecke, and O. Boric-Lubecke, "Data-based quadrature imbalance compensation for a CW Doppler radar system," *IEEE Transactions on Microwave Theory and Techniques*, vol. 61, no. 4, pp. 1718–1724, 2013.